

RESEARCH ARTICLE | JULY 02 2009

Cryogenic vacuum tribology of diamond and diamond-like carbon films

M. Aggleton; J. C. Burton; P. Taborek



J. Appl. Phys. 106, 013504 (2009)

<https://doi.org/10.1063/1.3158339>



Articles You May Be Interested In

Effecting of the counterface on the antifriction properties of ceramics based on zirconium dioxide

AIP Conference Proceedings (November 2022)

Friction and counterface wear influenced by surface profiles of plasma electrolytic oxidation coatings on an aluminum A356 alloy

J. Vac. Sci. Technol. A (September 2012)

The friction couples for operation in the fuel and hydraulic systems

AIP Conf. Proc. (March 2024)



Journal of Applied Physics

Special Topics Open
for Submissions

[Learn More](#)

Cryogenic vacuum tribology of diamond and diamond-like carbon films

M. Aggleton, J. C. Burton, and P. Taborek^{a)}*Department of Physics and Astronomy, University of California, Irvine, California 92697, USA*

(Received 5 January 2009; accepted 30 May 2009; published online 2 July 2009)

Friction measurements have been performed on microcrystalline, ultrananocrystalline, and diamond-like carbon (DLC) films with natural diamond counterfaces in the temperature range of 8 K to room temperature. All films exhibit low friction ($\mu \leq 0.1$) in air at room temperature. In ultrahigh vacuum, microcrystalline diamond quickly wears into a high friction state ($\mu \approx 0.6$), which is independent of temperature. DLC has low friction even at the lowest temperatures. In contrast, friction in ultrananocrystalline films has a significant temperature dependence, with a broad transition from a low to a high friction state between 120 and 220 K observed on both heating and cooling. The role of hydrogen transport in determining the temperature dependence of friction is discussed. © 2009 American Institute of Physics. [DOI: 10.1063/1.3158339]

I. INTRODUCTION

Diamond and diamond-like carbon (DLC) films are tribologically useful coatings due to their typically low coefficient of friction.^{1–4} They are used as coatings in macroscopic objects such as engine parts⁵ and disk drives,⁶ and in the construction of microelectromechanical systems (MEMS).^{7,8} Diamond films deposited using chemical vapor deposition (CVD) are grown from plasmas, which contain a variable concentration of atomic and molecular hydrogen and various CH_x species.⁹ This intrinsically nonequilibrium growth process can yield a wide range of materials with different grain sizes, sp^2/sp^3 ratios, and hydrogen concentrations, which are determined by details of the growth process parameters. Grain size is a simplistic but nevertheless useful way to classify diamond films. Microcrystalline diamond (MCD), ultrananocrystalline diamond (UNCD), and DLC are often used to denote films with micron, nanometer, and atomic scale orders, respectively. This classification is useful because there is a general tendency for sp^2 (graphitic) content and hydrogen concentration to increase as the grain size decreases.

Although friction in diamond has been intensively studied, most previous measurements of diamond friction have been performed at room temperature or above, in the presence of air or some other lubricant, and often with a nondiamond counterface.^{10–13} Our main focus is the study of the friction of diamond/diamond sliding interfaces in vacuum as a function of temperature from room temperature to cryogenic temperatures. Our interest is motivated by possible applications of MEMS devices in extreme environments, as well as the more basic question of the behavior of self-mated dry friction at very low temperature.

Diamond is an interesting material for this study because of its very high Debye temperature of 1860 K. This implies that most of the phonon modes that contribute to the heat capacity are frozen out in diamond even at room temperature, and the thermodynamic properties become increasingly nonclassical as the temperature is lowered. The only previ-

ous studies of friction in diamond at low temperatures utilized diamond samples in contact with fluid cryogens.¹⁴ Diamond on diamond friction measurements in vacuum and low pressure environments at room temperature^{1,15–17} showed that tribological properties often degrade in ultrahigh vacuum (UHV), and hydrogen plays a special role in maintaining low friction coefficients in diamond. Molecular dynamics (MD) simulations have also been used to model friction between two diamond surfaces.^{18–22} In these studies, friction increased slightly as the temperature was lowered from 300 to 50 K, and increases rapidly below 50 K. This is presumably due to the difference in thermal motion of the atoms in the simulation at these different temperatures, although there is no obvious physical mechanism to explain a sharp transition near 50 K. The applicability of the classical MD in this temperature range where quantum effects are important is not clear.

The experiments reported here utilized different types of diamond films with a wide range of grain size, initial roughness, and hydrogen content. These experiments were performed using a sliding block tribometer, which was compatible with UHV and cryogenic temperatures. Measurements were performed in air and under vacuum to evaluate “run-in” behavior. The temperature dependence of the kinetic friction coefficient in UHV was measured in the range 8–300 K. We find that DLC films with high hydrogen content have low values of friction ($\mu_k < 0.1$) while microcrystalline films with relatively low hydrogen content had high values of friction ($\mu_k \approx 0.5$) throughout this temperature range, with very little temperature dependence. Ultrananocrystalline films had an intermediate behavior, with low friction at room temperature but high friction at low temperature, with the crossover taking place at approximately 170 K.

II. EXPERIMENTAL

Kinetic friction measurements were performed using the sliding block tribometer described in Ref. 23. Briefly, a high speed video is used to monitor the motion of a copper block supported by natural diamond tips sliding down a vee-shaped track. The track is formed from two pieces of diamond

^{a)}Electronic mail: ptaborek@uci.edu.

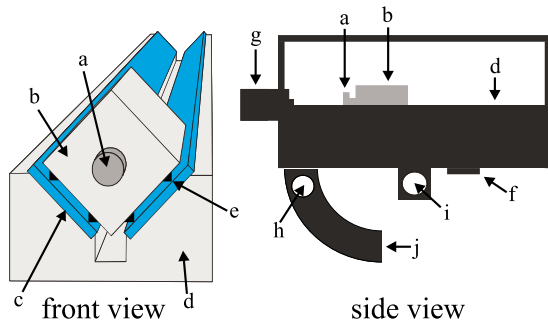


FIG. 1. (Color online) Schematic of sliding tribometer: (a) μ -metal button, (b) copper slider, (c) diamond coated tracks, (d) copper vee-track base, (e) natural diamond counterfaces, (f) thermometer, (g) solenoid, (h) heater, (i) pivot, and (j) counterweight.

coated silicon with dimensions of $10 \times 1.25 \text{ cm}^2$ (Fig. 1). The diamond tips on the sliding block were removed from commercial diamond scribes (J&M Diamond Tool, Inc.) and are initially conical in shape with a 90° angle at the tip. After only a few cycles the tips wear down to truncated cones with a circular flat on the end of radius $35 \pm 25 \text{ }\mu\text{m}$, as shown in Fig. 2. This radius is used to calculate a contact pressure of approximately 10–60 MPa for a block with mass of 30 g (depending on the tilt angle of the tribometer and specific wear on each tip). The tribometer is mounted in a vacuum can with several optical windows, which forms the outer part of the cryostat. To make a friction measurement, a solenoid at one end of the vee-track is activated, which magnetically attracts a small μ -metal button on the end of the slider to keep it pinned to the end of the track. μ -metal was chosen because it has no remaining magnetization after being removed from a magnetic field; thus there will be no issues with eddy currents during the descent of the block. The vee-track is then rotated into position so that the block will slide when the solenoid is released. As the solenoid is disengaged, a high speed video camera (Phantom 7.2) is triggered to capture the slide at a rate of 1000 fps. Spring loaded bumpers at the ends of the track reduce the vertical bouncing caused by impact at the end of the track. During the slide, the block moves under the influence of gravity and frictional forces, which produce a constant acceleration, so the displacement

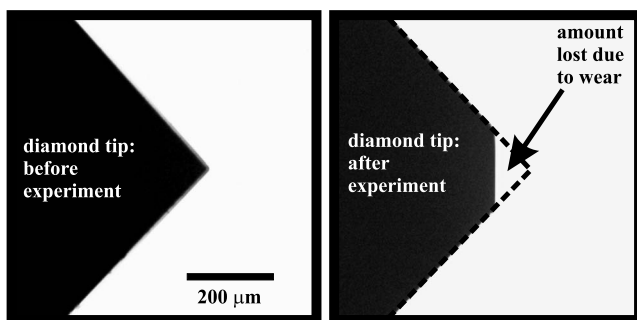


FIG. 2. Optical micrograph of the diamond tips, which slide across the diamond film substrates. The tips are 90° cones, which initially end in a sharp point with a $10 \text{ }\mu\text{m}$ radius, as shown on the left. After an experimental run, the tips wear into a truncated cone with a typical radius of $35 \pm 25 \text{ }\mu\text{m}$. Most of this wear occurs in the initial run-in period. The tip shown on the right was cycled thousands of times to make the worn region more obvious.

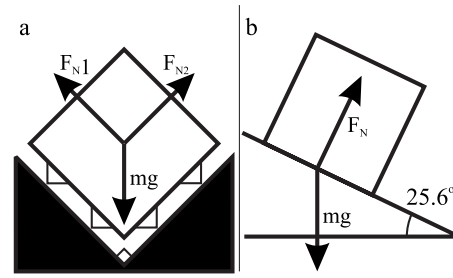


FIG. 3. The normal force on the block from the track has contributions from (a) the vee-track shape and (b) the angle the track is tilted for the block to slide. This contributes factors of $\sqrt{2}$ and $\cos \theta$, respectively, giving a total normal force of $F_N = \sqrt{2}mg \cos \theta$.

of the block is a quadratic function of time. Videos of the motion are analyzed using an edge tracking software to measure the position of the block as a function of time, and the acceleration of the block is calculated by fitting a parabola to the trajectory. The total normal force on the block is

$$F_N = \sqrt{2}mg \cos \theta, \quad (1)$$

where m is the mass of the block, g is the acceleration due to gravity, and θ is the angle that the track is tilted from the horizontal (Fig. 3). The factor of $\sqrt{2}$ arises from the vee-track and the $\cos \theta$ from the angle to which the track is tilted for the block to slide. The total normal force is 0.18 N, or 0.036 N per point of contact, assuming 5 points of contact. Using this normal force and the acceleration of the block down the track, the coefficient of kinetic friction can be calculated via Newton's second law. The coefficient of kinetic friction, μ_k , is

$$\mu_k = \frac{1}{\sqrt{2} \cos \theta} \left(\sin \theta - \frac{a}{g} \right), \quad (2)$$

where a is the measured acceleration, g is the acceleration due to gravity, and θ is the angle of the track with respect to the horizontal. After each slide, the track is immediately reset to return the slider to the starting position to wait for the next measurement, although the solenoid is not engaged until it is time to measure the next data point so as to not heat the slider.

The diamond films were between 2 and 3 μm thick and were produced by CVD on silicon substrates by commercial vendors. The MCD was produced by sp3, Inc., the DLC by Morgan Advanced Ceramics, and the UNCD by Advanced Diamond Technologies, Inc., which provided two samples denoted UNCD1 and UNCD2 and were manufactured with a slightly different process and thus had different hydrogen contents while other film properties remained the same. The hydrogen content, grain size, and roughness of these films are described in Table I. The grain size of DLC is not listed because DLC does not contain diamond grains but is an amorphous mixture of sp^2 and sp^3 bonded carbon atoms. The hydrogen content was measured using hydrogen forward scattering by Evans Analytical Group. Large grain size and high initial roughness are correlated with low hydrogen content.

Each friction measurement was begun with fresh, sharp, diamond tip counterfaces on the sliding block. The initial

TABLE I. Diamond film characteristics. Roughness values, measured before friction tests, have no effect on friction after initial run-in. Surface hydrogen content is for the top 500 nm of the film. All films are deposited on silicon wafers and are 2 μm thick except for MCD, which is 3 μm thick.

Diamond type	Hydrogen content	Grain size	Initial roughness (nm)
Microcrystalline diamond (MCD)	3.2% at the surface and 1.1%–1.9% in bulk	1–2 μm	300
Ultrananocrystalline diamond (UNCD1)	4.8% at the surface and 3.8% in bulk	3–5 nm	10
UNCD2 with high H content	7.7% overall	3–5 nm	10
Diamondlike carbon (DLC)	25% overall	N/A	14

surface roughness of the films varies over a wide range, but the wear-in process significantly alters the topography. The surfaces were worn in by sliding up to several hundred times in air at room temperature. In agreement with previous results,^{24,25} this procedure lowers the friction coefficient and generates a steady state friction value, which becomes independent of cycle number as shown in Fig. 4. Although the exact value at which the friction coefficient plateaus is dependent on the material parameters of the substrate and the counterface, as well as on the residual roughness of the wear track,²⁵ the focus of our investigation is the temperature dependence of this steady state value on the friction coefficient. After the room temperature wear-in procedure, the apparatus was pumped out and the cooldown was initiated. The cryostat consisted of several concentric radiation shields, as shown in Fig. 5, with independent control over the tribometer temperature. As the inner radiation shield was cooled to its operating temperature of 8 K (which takes approximately 12 h), the temperature of the tribometer was maintained at 295 K, which effectively cryopumps the tribological surfaces. The vacuum environment of our apparatus is rather unusual. Conventional UHV surface spectroscopies are not compatible with our cryogenic setup. Even an ion gauge would generate too high a heat load onto the 8 K shield, so the pressure cannot be measured directly. Nevertheless, the effective pressure in our apparatus is far below the values of 10^{-10} Torr typical of room temperature UHV systems. The tribometer is completely surrounded by surfaces at 8 K, which permanently trap all species except helium, so it is effectively inside a cryopump. Similar systems in our laboratory have been used to keep extremely reactive surfaces such as cesium and rubidium atomically clean for

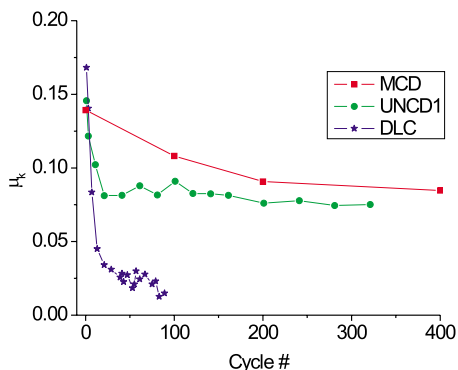


FIG. 4. (Color online) Friction coefficient as a function of cycle number for various types of diamond film substrates in air at room temperature. The plot shows that DLC undergoes the largest and fastest run-in process, while MCD undergoes the smallest and slowest change.

months.^{26,27} Although water vapor can have a significant effect on the tribological behavior of various materials,²⁸ water is not an issue in this experiment. As has been observed in several studies,^{29–31} water rapidly desorbs between 130 and 180 K from many surfaces including Rh, Ag, and graphite. By holding the temperature of the experiment at 295 K for several hours while preparing the cryogenic UHV environment, the coverage of water on the tribological surfaces is reduced to negligible levels.

The sliding block came into mechanical contact with the track only through the diamond load points and the μ_k metal button, so its thermal connection to the track was rather weak. The effective temperature of the block was determined in a separate calibration run-in which a thermometer was attached to its top surface. The temperature of the block was typically within approximately 15 K of the temperature of the track, but the sign of the difference and the exact value depended on the rate of heating or cooling and the absolute temperature. The temperature measured in the calibration run was used to establish the coupling parameters in a thermal model, which included conductive and radiative heat transfer and the temperature dependent heat capacity of the block. Because of the small contact area, radiation is the dominant mode of heat transfer to and from the block. The results of the model were verified for a wide range of heating and cooling rates. For all subsequent runs, the thermometer on the sliding block was removed, and its temperature was determined from the model using the known temperature and heating or cooling rate of the track.

The model provided the average temperature of the sliding block, but it did not account for the instantaneous and localized heating due to friction at the contact points. We estimated this so-called “flash temperature” by solving the

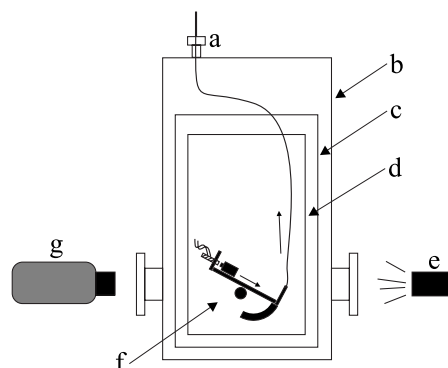


FIG. 5. Schematic of cryostat: (a) vacuum feedthrough, (b) vacuum can, (c) 40 K shield, (d) 4 K shield, (e) spotlight, (f) sliding tribometer, and (g) high speed camera.

one dimensional heat diffusion equation for an infinite rod with a heat flux at one end proportional to velocity and the coefficient of friction. Approximating the diamond tip as a thin rod with a contact area of $1.2 \times 10^{-9} \text{ m}^2$ in this way will have the effect of overestimating the contact temperature. The solution for the temperature rise at the contact point ΔT is³²

$$\Delta T = \frac{2t^{3/2}a\sqrt{\chi}}{3\kappa\sqrt{\pi}}, \quad (3)$$

where t is the time duration of the slide, which was 0.2 s in this case; χ is the thermal diffusivity of diamond, which ranges from 0.007 to $3 \text{ m}^2/\text{s}$ as a function of temperature; κ is the thermal conductivity of diamond, which ranges from 1 to 100 W/m K ; and a is the constant acceleration of the block. The infinite rod solution is valid for times less than the thermal diffusion time L^2/χ , where L is the length of the diamond tip; this characteristic time is less than 0.2 s for our system. Since the slide time is comparable to the thermal diffusion time in diamond, the diamond tip can be assumed to be approximately isothermal, and the heat flux out of the tip is limited by the thermal properties of the steel base, which the diamond tip is mounted to. The calculation made for steel produces a ΔT of 0.02–2.0 K. The same calculation for infinite diamond yields a ΔT of 0.11–0.54 K. The actual ΔT is expected to be between these two sets of values. We conclude that local frictional heating is a negligible correction to the average measured temperature in our system, but this is only true because of the short duration of the slide. In conventional tribometers that use continuous rotational motion, it is common to have flash temperatures of several hundred Kelvin.^{33,34}

Within the UHV environment, the tribometer temperature could be controlled between 295 and 8 K. Friction measurements were obtained as the sample was cooled to its lowest temperature, as well as when the sample was heated back to 295 K to check for hysteresis and wear. Approximately 200 slides in UHV were performed for each sample.

III. RESULTS

All types of diamond films tested had qualitatively similar wear-in behavior in air at room temperature. As has been seen elsewhere,³⁵ initially high friction quickly dropped to a lower value, which remained constant as long as the film remained in air at room temperature. The coefficient of friction, in all cases, began between 0.14 and 0.17 and decreased to low values of 0.09 or less. MCD required the longest run-in, while DLC required only 13 sliding cycles to reach its asymptotic low friction state, as shown in Fig. 4.

As the air was pumped out of the apparatus and the samples reached UHV conditions at room temperature, the friction properties of DLC and UNCD showed essentially no change, maintaining their low friction value. In contrast, the MCD sample's coefficient of friction rapidly increased over approximately 100 cycles from $\mu_k=0.065$ to $\mu_k=0.7$, as shown in Fig. 6. Similar behavior was observed by Feng *et al.*¹ Subsequent inspection of the wear track showed that this transition from low to high friction was accompanied by sig-

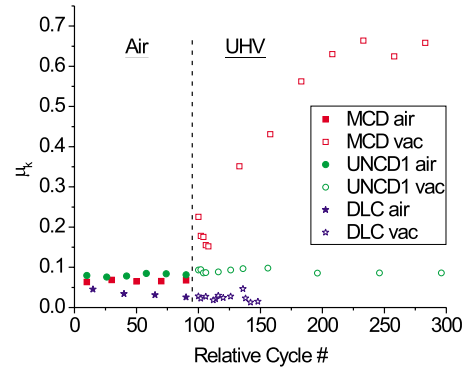


FIG. 6. (Color online) Friction coefficient as a function of relative cycle number at room temperature, showing the effects of pressure. The points to the left of the dotted line are obtained in atmospheric air after the run-in process observed in Fig. 4. The points to the right of the dotted line (UHV, $P \approx 10^{-6}$ Torr) are shifted to begin at cycle 100. Only MCD (lowest hydrogen content) is affected by vacuum.

nificant wear. In one experiment, a MCD sample was worn in at room temperature in air, after which no slides were performed until the tribometer had reached its bottom temperature of 10 K. At this low temperature, only 8 sliding cycles were required to make the transition from low to high friction, as shown in Fig. 7. In addition, friction returned to a low value immediately upon return to an air atmosphere, as has been seen previously.³⁶

The temperature dependence of the friction coefficient for each type of diamond film is shown in Fig. 8. Both the MCD and the DLC samples had very little temperature dependence. After UHV wear-in, the MCD samples had high friction $\mu_k > 0.5$ and μ_k increased only slightly to $\mu_k=0.6$ as the temperature was lowered to 8 K. The DLC sample maintained a low value of $\mu_k < 0.1$ down to the lowest temperatures investigated; above $T=180 \text{ K}$, the friction is particularly low and shows no thermal hysteresis. In contrast, the friction coefficient for the UNCD films depends strongly on temperature. At room temperature, the UNCD films have values of μ_k in the range of 0.1, but as the temperature is reduced, μ_k rises to 0.35. The transition from low to high friction takes place in the temperature interval between 150 and 225 K. Although there are some hysteresis and scatter in

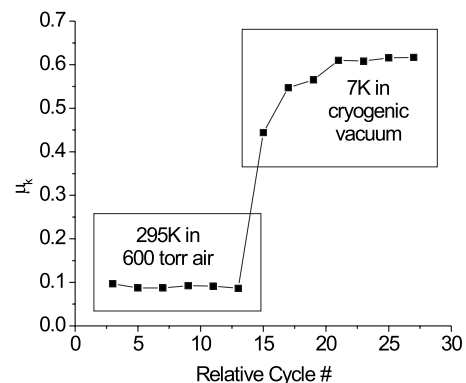


FIG. 7. Friction coefficient of MCD as a function of relative cycle number. The sample was worn in a room temperature in air. No further sliding cycles were performed until the sample reached 7 K under cryogenic vacuum. At low temperature, less than 10 sliding cycles were required to reach a steady state high friction state.

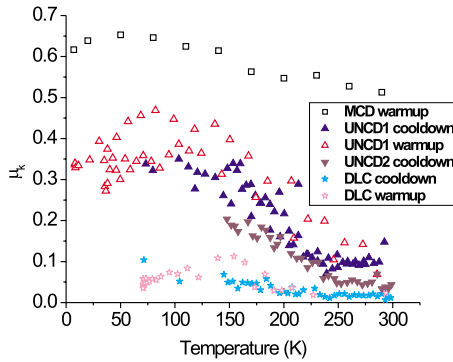


FIG. 8. (Color online) Friction coefficient for several types of diamond substrate as a function of temperature. The friction is similar for both cooling and heating runs for all materials. The friction for MCD is high and for DLC low, and both have only a weak temperature dependence, with a slight tendency toward higher friction at low temperature. The friction in UNCD makes a reversible transition between high and low friction states in the temperature range of 120–220 K. All measurements under cryogenic vacuum.

the friction measurements, this transition is essentially reversible, with the sample returning to a low friction state at $T=295$ K after a complete thermal cycle.

The data shown in Fig. 8 were obtained by observing one slide at each new value of the temperature. In an attempt to separate the effects of temperature from wear-in and the total number of sliding cycles on the transition observed for the UNCD samples, we performed several experiments in which the sample was abruptly dropped from room temperature to a constant temperature within the transition region after measuring a base-line friction level at room temperature. The friction coefficient was then measured for 40–70 sliding cycles at a fixed temperature. The results are shown in Fig. 9. The rate of increase in the coefficient of friction was observed to be identical at 228 and 206 K. The final coefficient of friction, however, was notably different. Near the beginning of the transition, at 228 K, the coefficient of friction began to level out at 0.32 after approximately 25 cycles. However, at 206 K, well into the thermal transition, friction only appeared to begin to level out at 0.6 after ap-

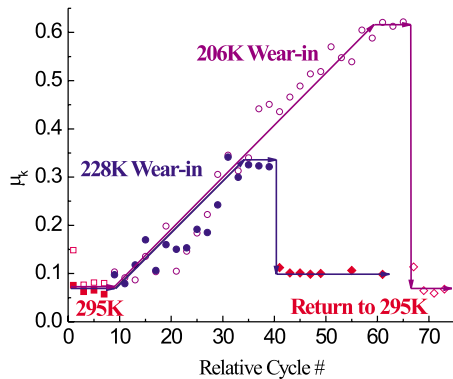


FIG. 9. (Color online) Friction coefficient of UNCD1 plotted vs relative cycle number at constant temperatures near the beginning temperature of the observed friction rise regime as seen in Fig. 8. Friction was measured at 295 K, then at lower temperature (228 or 206 K), then again at 295 K. The arrows indicate time progression, but are not linear fits to the data. Data were taken after temperature cycling (Fig. 8) but before breaking cryogenic vacuum. All measurements under cryogenic vacuum.

proximately 50 cycles. The final value for 206 K may actually be higher, but the experiment was stopped at this point to prevent excessive film damage. In each case, the tribometer was then returned to 295 K and friction was measured several times. In both cases the friction coefficient returned to its low state, confirming that the observed effect is dependent on temperature and not a result of permanent wear or film damage.

Wear is important, however, in determining the turnover rate of material at the sliding surfaces. Quantitative measurements of the wear of the films were difficult because the wear is small and spatially inhomogeneous. In MCD, wear takes place primarily at the highest asperities, which produce mesas in the film in an irregular pattern. In UNCD and DLC films, the wear track is almost invisible except for isolated regions where micron size pieces of material have been removed. Because of the well-defined geometry, it is much easier to measure the wear on the conical diamond tips on the block, which made contact with the films on the track. The tips had an initial radius of approximately $10 \mu\text{m}$, but wear to approximately $35 \pm 25 \mu\text{m}$ (Fig. 2) at the end of an experimental run. The total worn volume varies from approximately 10^{-13} to $2 \times 10^{-14} \text{ m}^3$. For our loads and track lengths, this wear volume is equivalent to a wear rate of $10^{-5} \text{ mm}^3/\text{N m}$, which is in good agreement with previous measurements of diamond on diamond wear in vacuum.³⁷ Assuming that the wear volumes of the tip and the substrate are equal yields an average track depth of 10^{-8} – 10^{-7} m . This rate of wear corresponds to approximately 0.01–0.1 atomic layers removed per sliding cycle.

IV. DISCUSSION AND CONCLUSION

Although the tribological behaviors of MCD, UNCD, and DLC are rather similar in air at room temperature, their behaviors in vacuum and at cryogenic temperatures are distinctly different. In vacuum at room temperature, MCD wears within 10–100 sliding cycles into a state with $\mu \approx 0.6$. This high friction state is essentially independent of temperature down to the lowest temperatures investigated. For DLC at room temperature, the performances in air and vacuum are identical, with $\mu \approx 0.03$ independent of the number of cycles. As the temperature is lowered, μ remains constant down to approximately 200 K. As the temperature is lowered further, μ increases slightly but remains below 0.1. UNCD samples are also unaffected by vacuum at room temperature, with μ in the range 0.05–0.15. μ remains constant down to $T \approx 230$ K. As the temperature is decreased, μ rises until it plateaus around 100 K at a value of $\mu \approx 0.3$ –0.4.

Numerous previous investigations have established that hydrogen plays an important role in determining the friction of diamond and DLC surfaces.^{15,17,38} In air, diamond and DLC surfaces are terminated with hydrogen, and the repulsive interactions between the C–H bonds on two sliding diamond surfaces lead to low friction.^{4,39,40} The topmost hydrogen terminated layers are worn away at a rate in the range 10^{-4} – 10^{-1} layers/cycle, depending on the details of the load and the material. If the hydrogen termination is not replenished, the subsequent sliding involves dangling carbon bonds

in direct contact, which leads to high friction. This picture implies that maintaining a low friction state requires a source of hydrogen, which can compensate for the hydrogen removed by wear; the hydrogen source can be either from the gas phase, transported on the surface, or through the bulk of the solid.

For MCD, the fact that the friction can be reversibly modulated with changes in gas pressure implies that the source of hydrogen is the ambient gas. In high vacuum at room temperature and below, the transport rate of hydrogen through or across the surface of the solid is so slow that it cannot compensate for wear on any conventional experimental time scale. Although the hydrogen content of UNCD is within a factor of 2–3 of MCD, its tribological behavior in vacuum and at low temperatures is dramatically different, which suggests a corresponding difference in the hydrogen transport mechanism. In UNCD, transport of hydrogen in the solid is apparently rapid enough to replenish the hydrogen across a wear track with a characteristic scale of $\approx 50 \mu\text{m}$ within a few seconds. Moreover, the hydrogen transport mechanism is temperature dependent. In the temperature range 170–230 K, μ rises from ≈ 0.1 to ≈ 0.3 , which suggests that the rate of hydrogen transport has decreased so much that below 170 K it can no longer compensate for wear. It is noteworthy that the hydrogen transport mechanism is unlikely to be conventional bulk diffusion through the diamond lattice. Although bulk diffusion of hydrogen through diamond is a thermally activated process, the activation energy is $\approx 2 \text{ eV}$, $\approx 22\,000 \text{ K}$, and the diffusion rates are negligibly small even at room temperature.⁴¹ If diffusive transport of hydrogen is indeed responsible for the temperature dependence of the friction in UNCD, then the activation energy must be only a few hundred kelvin. The process with activation energies of this size has been identified in studies of low temperature internal friction of diamond.⁴² It is intriguing to speculate that the difference in friction behavior in MCD and UNCD is related to transport along grain boundaries. Although the hydrogen content varies by less than an order of magnitude, the grain size of MCD and UNCD differs by three orders of magnitude.

The tribological properties of DLC are not easily explained by the hydrogen transport picture. DLC is 25% hydrogen, which is approximately three to five times greater than our UNCD samples. DLC has a very low $\mu \approx 0.03$ at room temperature in both air and vacuum. This low value persists down to $T \approx 170 \text{ K}$ where μ roughly doubles and then remains constant down to the lowest temperatures investigated. Although the characteristic temperature for the increase in friction is approximately the same as for UNCD, the asymptotic low temperature value of μ is much lower. If transport through grains plays a role, it seems to be much less important in DLC than in UNCD. Perhaps the bulk concentration of hydrogen in DLC is high enough that fresh surface exposed by wear can be hydrogen terminated without requiring long range motion of hydrogen. In any case, DLC films have the mechanical integrity to survive thermal cycling and have excellent wear and friction properties in vacuum at cryogenic temperatures.

ACKNOWLEDGMENTS

We thank J. Krim, K. J. Wahl, and J. A. Harrison for useful discussions. This work has been supported by EXTREME FRICTION AFOSR MURI Grant No. FA9550-04-1-0381.

- ¹Z. Feng, Y. Tzeng, and J. E. Field, *J. Phys. D* **25**, 1418 (1992).
- ²R. Hauert, *Tribol. Int.* **37**, 991 (2004).
- ³Y. Liu, A. Erdemir, and E. I. Meletis, *Surf. Coat. Technol.* **94-95**, 463 (1997).
- ⁴A. R. Konicek, D. S. Grierson, P. U. P. A. Gilbert, W. G. Sawyer, A. V. Sumant, and R. W. Carpick, *Phys. Rev. Lett.* **100**, 235502 (2008).
- ⁵A. Lettington, *Carbon* **36**, 555 (1998).
- ⁶P. R. Goglia, J. Berkowitz, J. Hoehn, A. Xidis, and L. Stover, *Diamond Relat. Mater.* **10**, 271 (2001).
- ⁷T. Shibata, Y. Kitamoto, K. Unno, and E. Makino, *J. Microelectromech. Syst.* **9**, 47 (2000).
- ⁸J. P. Sullivan, T. A. Friedmann, and K. Hjort, *MRS Bull.* **26**, 309 (2001).
- ⁹D. S. Grierson and R. W. Carpick, *Nanotoday* **2**, 12 (2007).
- ¹⁰S. E. Grillo and J. E. Field, *J. Phys. D* **33**, 595 (2000).
- ¹¹S. E. Grillo and J. E. Field, *Wear* **254**, 945 (2003).
- ¹²F. Gao, A. Erdemir, and W. T. Tysoc, *Tribol. Lett.* **20**, 221 (2005).
- ¹³H. I. Kim, J. R. Lince, O. L. Eryilmaz, and A. Erdemir, *Tribol. Lett.* **21**, 51 (2006).
- ¹⁴Y. Iwasa, A. F. Ashaboglu, E. R. Rabinowicz, T. Tachibana, and K. Kobashi, *Cryogenics* **37**, 801 (1997).
- ¹⁵A. Erdemir, O. L. Eryilmaz, and G. Fenske, *J. Vac. Sci. Technol. A* **18**, 1987 (2000).
- ¹⁶J. Fontaine, C. Donnet, A. Grill, and T. Le Mogne, *Surf. Coat. Technol.* **146-147**, 286 (2001).
- ¹⁷J. Fontaine, M. Belin, T. Le Mogne, and A. Grill, *Tribol. Int.* **37**, 869 (2004).
- ¹⁸J. A. Harrison, C. T. White, R. J. Colton, and D. W. Brenner, *Phys. Rev. B* **46**, 9700 (1992).
- ¹⁹J. A. Harrison, C. T. White, R. J. Colton, and D. W. Brenner, *Thin Solid Films* **260**, 205 (1995).
- ²⁰J. A. Harrison, R. J. Colton, C. T. White, and D. W. Brenner, *Wear* **168**, 127 (1993).
- ²¹G. T. Gao, R. J. Cannara, R. W. Carpick, and J. A. Harrison, *Langmuir* **23**, 5394 (2007).
- ²²M. J. Brukman, G. T. Gao, R. J. Nemanich, and J. A. Harrison, *J. Phys. Chem. C* **112**, 9358 (2008).
- ²³J. C. Burton, P. Taborek, and J. E. Rutledge, *Tribol. Lett.* **23**, 131 (2006).
- ²⁴S. Achanta, D. Drees, and J. P. Celis, *Wear* **259**, 719 (2005).
- ²⁵I. P. Hayward, I. L. Singer, and L. E. Seitzman, *Wear* **157**, 215 (1992).
- ²⁶J. E. Rutledge and P. Taborek, *Phys. Rev. Lett.* **69**, 937 (1992).
- ²⁷J. A. Phillips, D. Ross, P. Taborek, and J. E. Rutledge, *Phys. Rev. B* **58**, 3361 (1998).
- ²⁸A. J. Haltner, and C. S. Oliver, *I&EC Fundamentals* **5**, 348 (1966).
- ²⁹A. Beniya, S. Yamamoto, K. Mukai, Y. Yamashita, and J. Yoshinobu, *J. Chem. Phys.* **125**, 054717 (2006).
- ³⁰S. M. Dounce, S. H. Jen, M. Yang, and H. L. Dai, *J. Chem. Phys.* **122**, 204703 (2005).
- ³¹D. V. Chakarov, L. Österlund, and B. Kasemo, *Vacuum* **46**, 1109 (1995).
- ³²H. S. Carslaw and J. C. Jaeger, *Conduction of Heat in Solids* (Clarendon, Oxford, 1978).
- ³³F. P. Bowden and D. Tabor, *The Friction and Lubrication of Solids* (Clarendon, Oxford, 1950).
- ³⁴J. C. Jaeger, *J. Proc. R. Soc. N. S. W.* **76**, 203 (1943).
- ³⁵M. N. Gardos and B. L. Soriano, *J. Mater. Res.* **5**, 2599 (1990).
- ³⁶H. Guo, Y. Qi, and X. Li, *Appl. Phys. Lett.* **92**, 241921 (2008).
- ³⁷K. Miyoshi, *ASME J. Tribol.* **120**, 379 (1998).
- ³⁸S. Miyake, S. Takahashi, I. Watanabe, and H. Yoshihara, *ASLE Trans.* **30**, 121 (1987).
- ³⁹H. Zaidi, T. Le Huu, and D. Paulmier, *Diamond Relat. Mater.* **3**, 787 (1994).
- ⁴⁰T. Le Huu, H. Zaidi, and D. Paulmier, *Wear* **181-183**, 766 (1995).
- ⁴¹E. Vainonen, J. Likonen, T. Ahlgren, P. Haussalo, J. Keinonen, and C. H. Wu, *J. Appl. Phys.* **82**, 3791 (1997).
- ⁴²A. B. Hutchinson, P. A. Truitt, K. C. Swab, L. Skaric, J. M. Parpia, H. G. Craighead, and J. E. Butler, *Appl. Phys. Lett.* **84**, 972 (2004).